*Journal of Zhejiang University-SCIENCE B (Biomedicine & Biotechnology)* 2022 23(5):365-381
www.jzus.zju.edu.cn; www.springer.com/journal/11585
E-mail: jzus_b@zju.edu.cn

**Research Article**

https://doi.org/10.1631/jzus.B2100718



# Physicochemical properties, molecular structure, antioxidant activity, and biological function of extracellular melanin from *Ascosphaera apis*

Zhi LI[1,2,3]✉, Hui HENG[1], Qiqian QIN[1], Lanchun CHEN[1], Yuedi WANG[1], Zeyang ZHOU[1,4,5]

[1]*College of Life Sciences, Chongqing Normal University, Chongqing 401331, China*
[2]*Chongqing Key Laboratory of Vector Insects, Chongqing 401331, China*
[3]*Chongqing Key Laboratory of Animal Biology, Chongqing 401331, China*
[4]*Chongqing Key Laboratory of Microsporidia Infection and Control, Chongqing 400715, China*
[5]*The State Key Laboratory of Silkworm Genome Biology, Southwest University, Chongqing 400715, China*

**Abstract:** *Ascosphaera apis* spores containing a dark-colored pigment infect honeybee larvae, resulting in a large-scale collapse of the bee colony due to chalkbrood disease. However, little is known about the pigment or whether it plays a role in bee infection caused by *A. apis*. In this study, the pigment was isolated by alkali extraction, acid hydrolysis, and repeated precipitation. Ultraviolet (UV) analysis revealed that the pigment had a color value of 273, a maximum absorption peak at 195 nm, and a high alkaline solubility (7.67%) and acid precipitability. Further chemical structure analysis of the pigment, including elemental composition, Fourier transform infrared (FTIR) spectroscopy, Raman spectroscopy, mass spectrometry, and nuclear magnetic resonance (NMR), proved that it was a eumelanin with a typical indole structure. The molecular formula of melanin is $C_{10}H_6O_4N_2$, and its molecular weight is 409 Da. Melanin has hydroxyl, carboxyl, amino, and phenolic groups that can potentially chelate to metal ions. Antioxidant function analyses showed that A. apis melanin had a high scavenging activity against superoxide, hydroxyl, and 2,2-diphenyl-1-picrylhydrazyl (DPPH) radicals, and a high reducing ability to $Fe^{3+}$. Indirect immunofluorescence assay (IFA), scanning electron microscopy (SEM), and transmission electron microscopy (TEM) analyses showed that *A. apis* melanin was located on the spore wall. The spore wall localization, antioxidant activity, and metal ion chelating properties of fungal melanin have been suggested to contribute to spore pathogenicity. However, further infection experiments showed that melanin-deficient spores did not reduce the mortality of bee larvae, indicating that melanin does not increase the virulence of *A. apis* spores. This study is the first report on melanin produced by *A. apis*, providing an important background reference for further study on its role in *A. apis*.

**Key words:** Melanin; Molecular structure; Antioxidant activity; Subcellular localization; *Ascosphaera apis*

## 1 Introduction

Melanin is a heterogeneous polymer composed of complex polyphenols or steroidal heteropolyaromatic compounds (Jacobson, 2000). It has been identified in many animals. For example, the ink of a squid consists of a suspension of melanin particles (Fiore et al., 2004; Guo et al., 2014), and different types of melanin confer the appearance of black or red hair in animals (Menon et al., 1983; Césarini, 1990) and color feathers in birds (McGraw et al., 2005). Many fungal species can also synthesize melanin (Wheeler and Bell, 1988; Butler and Day, 1998). Functionally, melanin contributes to energy transduction (Dadachova et al., 2007) and radiation protection, and can be exploited in edible electronic devices (Kim et al., 2013). Melanin in melanocytes in the skin provides protection against sunlight and allows melanoma to resist therapeutic radiation (Hill, 1991). It shows in vitro activity against human immunodeficiency virus, inhibiting syncytium formation and revealing the cytopathic effects of the virus (Montefiori and Zhou, 1991). Insects can use melanin polymers to block the invasion of microorganisms (Richman and Kafatos, 1996; Nappi and Christensen, 2005). Melanin can protect fungi from

✉ Zhi LI, lizhicqnu@gmail.com
Zhi LI, https://orcid.org/0000-0003-1611-4873

Received Aug. 16, 2021; Revision accepted Jan. 4, 2022;
Crosschecked May 11, 2022

severe temperature fluctuations, high osmotic pressure, oxidative stress, ultraviolet (UV) and γ radiation, soil enzymatic lysis, low moisture, and nutrient deficiencies (Butler and Day, 1998). Melanins are important for fungal cell wall mechanical strength (Wang et al., 1995; Gómez et al., 2001; Nosanchuk and Casadevall, 2003, 2006; Zaragoza et al., 2008; Nosanchuk et al., 2015). In addition to protection, many studies have found that melanins in pathogenic fungi, such as *Aspergillus fumigatus*, *Aspergillus nidulans*, and *Cryptococcus neoformans*, can assist in invasion (Kwon-Chung et al., 1982; Dixon et al., 1989), shield the host from recognizing antigens and block the host's immune pathways (Hernández-Chávez et al., 2017), and chelate environmental metal ions (Fogarty and Tobin, 1996).

Research has indicated that fungal melanins can be divided into two main forms: dihydroxyphenylalanine (DOPA)-melanins and dihydroxynaphthalene (DHN)-melanins (Langfelder et al., 2003). However, the chemical structure of most fungal melanins is unknown because they are not suitable for crystallization or structural study due to their structural diversity, their combination with proteins, carbohydrates or lipids, and the insolubility of amorphous materials. The chemical structure of only a few fungal melanins has been identified (Ye et al., 2014; Sun et al., 2016a, 2016b; Liu et al., 2018). Therefore, melanins from many important pathogenic fungi remain to be identified.

*Ascosphaera apis* has attracted considerable attention recently. It can cause the deadly chalkbrood disease of bees (Spiltoir, 1955; Spiltoir and Olive, 1955), inflicting severe worldwide economic losses in beekeeping and seriously undermining the ability of bees to pollinate crops (Spiltoir, 1955; Spiltoir and Olive, 1955; Aronstein and Murray, 2010). In the life cycle of *A. apis*, spores enter the midgut of bee larvae by ingestion and remain dormant (Morse, 1978; Wynns et al., 2013). When the honeybee larvae develop to instars 4–5, the spores germinate. After the mycelia grow and penetrate the intestinal wall, new spores enter the blood cavity and spread to all the tissues of the larvae. Eventually, the hyphae expand and kill the larvae, resulting in the infected larvae becoming "mummified" (Bailey, 1968; Heath and Gaze, 1987). We recently found that within one week of continued development on in vitro potato dextrose agar (PDA) medium, the opposing mating types of *A. apis* mycelium turned from white to black and produced newborns containing dark-colored infectious melanized spores at the meeting point. The dead larvae infected by *A. apis* were blackened and "mummified" (Li Z et al., 2018). Our transmission electron microscopy (TEM) observations of subcellular structure showed that the spore wall of mature black spores appeared to have a melanin-producing cyst structure similar to that of other known fungi (Li et al., 2012). However, little is known about the physicochemical properties, chemical structure, or biological activity of pigments from *A. apis*. Whether the pigment from *A. apis* can play a role in the *A. apis* infection process needs further confirmation.

This study is the first to isolate and identify melanin from the pathogenic fungus *A. apis*. The solubility, color value, elemental composition, chemical structure, biological activity, subcellular localization, and antioxidant activity of the melanin were systematically and comprehensively investigated using UV-visible spectroscopy, infrared spectroscopy, Raman spectroscopy, gas chromatography with mass spectrometry (GC-MS), nuclear magnetic resonance (NMR) technology, scanning electron and TEM, and free radical scavenging analysis. In addition, the iron-chelating ability of melanin was further explored, and the relationship between melanin and spore infection ability was analyzed after using tricyclazole to inhibit melanin synthesis. This paper provides an important background reference for studying the nature of melanin in *A. apis* and its possible role in bee infection.

## 2 Materials and methods

### 2.1 Isolation and purification of *A. apis*

The *A. apis* CQ1 isolates in this study were obtained from the College of Life Sciences, Chongqing Normal University, China. *A. apis* was scraped from the surface of infected larval mummies of honeybees (*Apis mellifera*) and then cultured on PDA. After many generations of incubation, the mature and black spores of *A. apis* were isolated and purified using discontinuous Percoll gradient centrifugation, as previously described (Li Z et al., 2018).

### 2.2 Extraction and purification of *A. apis* pigment

Melanin was extracted from purified black mature spores of *A. apis*. Melanin extracted by an alkaline extraction and acid precipitation method was used for

the identification of structural, physical, and chemical characteristics, while the melanin "ghost" extraction from an enzymatic digestion method was used for morphological and cell localization observations. For the alkaline extraction and acid precipitation method, the purified *A. apis* spores were autoclaved at 120 ℃ for 30 min and ultrasonicated in phosphate-buffered saline (PBS) for 30 min using three 1-s bursts. Subsequently, the sample solution was adjusted to pH 10 with 1 mol/L NaOH and kept at 50 ℃ for 3 h. The solution was centrifuged at 12 000 r/min for 10 min to collect the supernatant. Then, melanin was purified by adjusting the pH to 1.0 with 6 mol/L HCl, and the solution was kept at 50 ℃ for 16 h. Melanin, collected after further centrifugation at 12 000 r/min for 20 min, was then successively washed with 0.01 mol/L HCl and distilled water. Finally, the purified melanin was freeze-dried and kept at −20 ℃ until further use.

For melanin "ghost" extracted by enzymatic digestion, purified *A. apis* spores were first mixed with 10 mg/mL novozyme (Sigma-Aldrich, Shanghai, China) and incubated overnight at 30 ℃ to generate protoplasts. The protoplasts were collected after centrifugation at 10000 r/min for 10 min. After washing three times with PBS, the sediment was suspended in 4.0 mol/L guanidine thiocyanate (Sigma-Aldrich, Shanghai, China) and then incubated overnight at room temperature. The dark-colored particles were collected after centrifugation at 10000 r/min for 10 min, washed three times with PBS, treated with 1.0 mg/mL proteinase K (Beyotime Biotechnology, Shanghai, China) in reaction buffer (10.0 mmol/L Tris, 1.0 mmol/L $CaCl_2$, and 0.5% (5 g/L) sodium dodecyl sulfate (SDS); pH 7.8) and lysing enzymes (containing β-glucanase, cellulase, protease, and chitinase; Merck KGaA, Darmstadt, Germany), and then incubated at 37 ℃ for 12 h. The dark-colored particles were washed three times with PBS and boiled in 6.0 mol/L HCl for 1.5 h. Melanin particles were collected after centrifugation at 12000 r/min for 10 min. Finally, the particles were washed and dialyzed with double-distilled water ($ddH_2O$) until the acid was completely removed, and then dried for use.

### 2.3 Physical and chemical characteristic analyses of *A. apis* pigment

#### 2.3.1 Solubility tests

*A. apis* melanin (10 mg) was weighed and mixed with 10 mL of each of the following solvents at room temperature: $ddH_2O$, $H_2O_2$, 1 mol/L NaOH, 1 mol/L HCl, methanol, anhydrous ethanol, ethyl ether, petroleum ether, glacial acetic acid, phosphoric acid, propionic acid, ammonia, glycerol, dimethyl sulfoxide, *n*-butanol, isoamyl alcohol, acetone, toluene, xylene, and trichloromethane. The solubility of *A. apis* melanin was observed after leaving the mixture to stand for 3 h.

#### 2.3.2 Determination of the color value

The color value of the *A. apis* pigment was determined as previously described (Ye et al., 2012; Raman and Ramasamy, 2017), and measured at 195 nm using a UV-visible spectrophotometer (Shimadzu 2100, Japan).

#### 2.3.3 UV-visible light absorption spectrum

The absorption properties of *A. apis* melanin were analyzed using UV-visible spectrophotometer (Shimadzu 2100, Japan). Absorption was recorded in the wavelength range of 180–900 nm using 0.1 mol/L NaOH solution as the reference.

#### 2.3.4 Elemental analysis

The percentages of C, H, N, O, and S contained in *A. apis* melanin were determined using an elemental analyzer (Euro Vector EA3000, Milan, Italy) as previously described (de la Rosa et al., 2017).

#### 2.3.5 Infrared spectrum analysis

Fourier transform infrared (FTIR) spectroscopy analysis was performed according to the method of Ye et al. (2014) with slight modifications. Briefly, *A. apis* melanin powder was ground and mixed with dry KBr (Sigma-Aldrich, Shanghai, China) in a 1:100 mass ratio, and then scanned with a 6700 FTIR spectrometer (Thermo Nicolet Co., Waltham, MA, USA) with a scanning range of 4000–400 $cm^{-1}$.

#### 2.3.6 Raman spectroscopy scanning

To explore the main functional groups in *A. apis* melanin, Raman spectroscopy analysis was carried out using a Renishaw Raman RM2000 spectrometer (Renishaw, Gloucestershire, UK) as previously described (de la Rosa et al., 2017; Galván et al., 2018).

#### 2.3.7 $^{1}$H-NMR and $^{13}$C-NMR analyses

$^{1}$H-NMR analysis was performed using a Bruker Avance AV-400 spectrometer (Bruker BioSpin GmbH, Rheinstetten, Germany) with reference to the method

of Ye et al. (2014). The conditions were as follows: temperature 300 K (26.85 ℃), delay time 1 s, and observation frequency 500.13 MHz. The sample was dissolved in NaOD, and chemical shifts are given in ppm (1 ppm=$1\times10^{-6}$). $^{13}$C-NMR analysis was performed using a Bruker Avance AV-500 spectrometer (Bruker BioSpin GmbH, Rheinstetten, Germany). The conditions refer to those of Ye et al. (2014): resonance frequency 130.255 MHz, using a 4-mm high-resolution magic angle spinning (HRMAS) probe and a spinning rate of 8 kHz, the number of scans 8192, and the delay time 1 s. The samples were dissolved in $D_2O$, and chemical shifts are given in ppm.

2.3.8 Electron paramagnetic resonance spectroscopy analysis

Electron paramagnetic resonance (EPR) spectral analysis of *A. apis* melanin was performed at the Analytical and Test Center of Chongqing University, Chongqing, China. Briefly, a 5-mg melanin sample was placed in a quartz EPR tube and frozen in liquid nitrogen. EPR spectra were recorded using a Bruker A300 spectrophotometer (Bruker Biospin GmbH, Rheinstetten, Germany), with the following parameters: microwave bridge frequency 9.85 GHz and power 19.12 mW; sweep width 100 G (1 G=0.1 mT), time 81.92 s and time constant 81.92 ms; modulation frequency 100 kHz and amplitude 1.00 G.

2.3.9 Pyrolysis GC-MS analysis

Pyrolysis GC-MS analysis was performed according to a the method of Ye et al. (2012). Finally, the samples were analyzed using GC-MS detection (Thermo Trace, Silicon Valley, USA). The parameters and conditions refer to those of a previous study (Ye et al., 2014) with minor modifications. Briefly, the oven temperature was set to 40 ℃ for 1 min, increased to 300 ℃ at a rate of 5 ℃/min, and then held for 10 min. The helium carrier gas was set to a flow rate of 1 mL/min. The injection volume was 1 μL and the split ratio was 40:1. In the mass spectrometer, the ion source temperature was 230 ℃, and the ionization mode was electron ionization (EI) of 70 eV.

**2.4 Biochemical activity of *A. apis* pigment**

2.4.1 Total antioxidant capacity assay

The ferric-reducing antioxidant power (FRAP) method for the total antioxidant capacity assay was carried out using the FRAP Plus kit (Beyotime Biotechnology, Shanghai, China) as previously described (Bao et al., 2021).

2.4.2 Superoxide radical scavenging activity assay

The pyrogallol oxidation method was used as previously described (Xu and Guo, 2008). Finally, the absorbance of sample ($A_{sample}$) at 318 nm was measured using a UV-visible spectrophotometer (Shimadzu 2100, Japan). Ascorbic acid was used as the control.

2.4.3 Hydroxyl radical scavenging activity assay

The antioxidant activity toward hydroxyl radical was detected as previously described (Chen et al., 2009), with minor modifications. Briefly, 1 mL of 0.75 mol/L 1,10-phenanthroline was mixed with 0.2 mmol/L PBS (pH 7.4, 2 mL) and 1 mL of $ddH_2O$. Then, 1 mL of 0.75 mmol/L ferrous sulfate ($FeSO_4$) and 1 mL of 0.01% (volume fraction) $H_2O_2$ were added to the mixture, followed by shaking and incubation at 37 ℃ for 60 min. Finally, the absorbance of the mixture at 536 nm was measured using a UV-visible spectrophotometer (Shimadzu 2100, Japan). The hydroxyl radical scavenging activity of the extract is expressed as a half maximal inhibitory concentration ($IC_{50}$) value.

2.4.4 2,2-Diphenyl-1-picrylhydrazyl (DPPH) radical scavenging activity assay

The DPPH radical scavenging activity of *A. apis* melanin was determined as previously described (Bersuder et al., 1998). The antioxidant activity of the extract is expressed as an $IC_{50}$ value, which was defined as the concentration (μg/mL) of extract that inhibits the formation of DPPH radicals by 50%.

2.4.5 $Fe^{2+}$ chelating activity assay

The $Fe^{2+}$ chelating activity assay was performed as previously described (Ye et al., 2012). The percent chelating rate was calculated according to the following formula: $Fe^{2+}$ chelating rate (%)=$(A_{blank}-A_{sample})/A_{blank}\times100\%$, where $A_{blank}$ is the absorbance of distilled water as a blank control and $A_{sample}$ is the absorbance of *A. apis* melanin.

**2.5 Preparation of antiserum against *A. apis* pigment**

According to a previous method (Li et al., 2012), *A. apis* melanin antiserum was generated by immunizing

mice with purified pigment ghost with appropriate modifications. Briefly, purified melanin ghost was mixed with Freund's adjuvant (1:1 (volume ratio); Sigma-Aldrich, USA) and injected using subcutaneous multipoint injection into three mice. One week after the third injection, the mice were bled and their sera were collected. Another three mice were immunized subcutaneously with multipoint injection of PBS to prepare negative antiserum.

### 2.6 Subcellular localization observation of *A. apis* pigment

#### 2.6.1 Scanning electron microscopy

For scanning electron microscopy (SEM), the extracted melanin "host" particles were treated as previously described (Li Z et al., 2018). Finally, the samples were transferred to an Emitech K850 critical point dryer (Emitech, East Sussex, UK) with liquefied carbon dioxide as the transitional fluid. The dried samples were gold-coated and transferred to SEM stubs. SEM investigations were performed with a Hitachi SU3500 scanning electron microscope (Tokyo, Japan).

#### 2.6.2 Transmission electron microscopy

For TEM analysis, the *A. apis* melanin "host" samples were treated as previously described (Li Z et al., 2018). Finally, ultrathin sections of 70–80 nm were cut with a Reichert Ultracut Ultramicrotome, stained with uranyl acetate followed by lead citrate, and viewed on a transmission electron microscope (FEI Tecnai Spirit, California, USA).

#### 2.6.3 Indirect immunofluorescence assay

*A. apis* melanin was analyzed using indirect immunofluorescence assay (IFA) according to our previous methods (Li et al., 2012). Finally, the spores were examined with an Olympus FluoView FV1000 confocal laser scanning microscope (Olympus, Tokyo, Japan).

### 2.7 Preparation of melanin-deficient spores of *A. apis*

Spores with functionally defective melanin were prepared by inhibiting melanin synthesis with tricyclazole or incubating spores with melanin antiserum. The preparation methods were as follows.

#### 2.7.1 Tricyclazole inhibitor method

Based on our previous culture method of *A. apis* (Li Z et al., 2018), 10 μg/mL tricyclazole was added to PDA (200 g/L peeled potatoes, 20 g/L agar, 10 g/L dextrose, and 5 g/L yeast extract). *A. apis* was cultured on this PDA medium at (30±5) ℃ and 80% relative humidity (RH). After many generations of incubation and isolation, the spores without melanin were purified using discontinuous Percoll gradient centrifugation, as reported in a previous study (Li et al., 2012).

#### 2.7.2 Melanin antiserum blocking method

Purified *A. apis* wild-type spores ($1\times10^5$ spores/mL) were incubated with *A. apis* melanin antiserum at 37 ℃ for 3 h at a ratio of 1:100 (volume ratio). Then, the spores were washed with PBS three times to remove excess antiserum and resuspended in PBS solution.

### 2.8 Rearing and survival analyses of honey bee larvae

A frame containing 1st-instar worker larvae from one honey bee colony was brought to the laboratory. Then, 240 1st-instar larvae were collected and raised individually in a standard 48-well cell culture plate (one bee/well), held in a dark incubator at (34.5±0.5) ℃ and 80% RH, and provided with sufficient food (mass fractions: 50% royal jelly, 6% fructose, 6% glucose, 2% yeast extract, and 36% dd$H_2O$) once a day. A total of 20 μL of diet was used for 3rd-instar larvae, 30 μL for 4th-instar larvae, 40 μL for 5th-instar larvae, and 50 μL for 6th-instar larvae. The larvae were divided into four groups for the infection experiment: a normal feeding control group, a wild-type spore infection group, a tricyclazole spore group (spores without melanin following tricyclazole culture), and an anti-melanin spore group (spores incubated with melanin antiserum). The detailed procedure was as follows: 4th-instar larvae were deprived of food for 4 h and then orally fed 20 μL of food containing one of the above three types of spores ($1\times10^5$ spores/bee), and the control group was fed normal food. Bees that consumed the entire test solution within 30 min were randomly selected and kept in a standard 24-well cell culture plate (one bee/well), held in a dark incubator at (35±1) ℃ with (65±5)% RH, and provided with sufficient food until they stopped feeding at the 6th instar. The survival of larvae was recorded daily. The mortality of honey bee larvae was analyzed in three replicates. According to Abbott's formula, mortality data were corrected and subjected to statistical survival

analysis using the Kaplan-Meier survival model with a log-rank test for overall comparison, using Statistical Package for Social Sciences (SPSS) v23.0 (SPSS Inc., Chicago, IL, USA).

### 2.9 Statistical analysis

The results were analyzed using SPSS v20.0 for Windows. All the data are expressed as the mean± standard error of the mean (SEM) from three independent biological repeats, with each composed of three technical repeats. Student's *t*-test was used to compare the means, and the values were considered significant at $P<0.05$.

## 3 Results

### 3.1 Optimum conditions for extracting *A. apis* melanin

The extraction of melanin depends on its solubility in alkaline solution and the formation of precipitates in acidic solution. Hydrolysis in acidic solutions can remove the proteins, carbohydrates, and lipids bound to melanin. In this study, *A. apis* melanin was extracted by the alkaline extraction and acid precipitation method. The maximum rate of production of *A. apis* melanin was 7.67%. The optimum hydrolysis temperature was 40–60 ℃ (Fig. S1a), and the optimum solid to liquid ratio was 1 g:10 mL (Fig. S1b). The extraction rate was positively correlated with the hydrolysis time of NaOH (Fig. S1c) and the concentration of HCl, but there was almost no change after the concentration of HCl increased to 6 mol/L (Fig. S1d).

### 3.2 Physicochemical properties and molecular structure of *A. apis* melanin

#### 3.2.1 Solubility and colority

*A. apis* melanin was easily soluble in alkaline solutions such as NaOH and ammonia, and had relatively high solubility in formic acid, phosphoric acid, and dimethyl sulfoxide. It was insoluble in common organic solvents such as chloroform, ethyl acetate, ethanol, propionic acid, acetic acid, ether, hexane, and acetone, but could be precipitated in mineral acid solutions such as HCl (Fig. S2). The colority of *A. apis* melanin was 273, which is close to that reported for melanin (Ye et al., 2012).

#### 3.2.2 UV-visible light absorption spectrum

UV-visible absorption spectrum analysis showed that the optical density of *A. apis* melanin gradually decreased with increasing wavelength. *A. apis* melanin had a maximum absorbance at 195 nm (Fig. S3). No absorption peaks between 260 and 280 nm were observed in the spectrum, suggesting that *A. apis* melanin did not contain nucleic acids, proteins, or lipids.

#### 3.2.3 Elemental composition

The elemental composition (mass fraction) of *A. apis* melanin was 42.18% C, 2.65% H, 6.40% N, 12.12% O, and 0.86% S (Fig. S4). The corresponding molar ratios of C:H, C:O, and C:N were 1.0:1.3, 4.6:1.0, and 7.7:1.0, respectively. Based on the defining characteristics of eumelanin (0.09% S) and phaeomelanin (9.78% S), DOPA-melanin (6%–11% N) and DHN-melanin (0% N), *A. apis* melanin contained 0.86% S and 6.40% N, indicating that *A. apis* melanin was primarily a DOPA-eumelanin. Moreover, the higher C:N ratio indicated that *A. apis* melanin did not contain amino groups, and the lower C:H ratio suggested that the pigment contained more heterocyclic structures (Schweitzer et al., 2009).

#### 3.2.4 EPR spectroscopy analysis

The EPR spectrum of pigment particles obtained from *A. apis* had a slightly asymmetric singlet with a full width at half maximum of the linewidth of EPR signal $\Delta B_{pp}$=4 G and the spectroscopic splitting factor $g$=2.005. The signal peak appeared at 3510 G of the EPR spectrum (Fig. 1), indicating that *A. apis* melanin contained a stable free radical compound, the defining feature of almost all reported melanins.

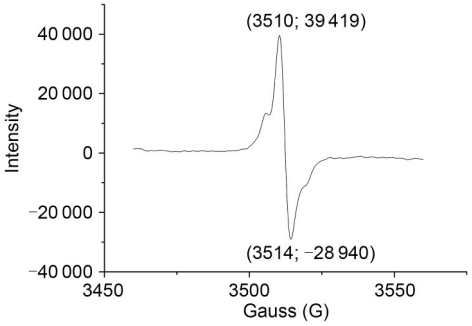


**Fig. 1 Electron paramagnetic resonance (EPR) spectroscopy analysis of melanin from *Ascosphaera apis*. 1 G= 0.1 mT.**

3.2.5 Infrared spectra

The results of infrared spectra analysis were shown in Fig. S5. Similar to other natural melanins, *A. apis* melanin had a wide range of broad absorption bands of 3500.0–3300.0 $cm^{-1}$ and a strong absorption peak at 3439.9 $cm^{-1}$, corresponding to the –OH and $–NH_2$ groups of the indole ring, respectively. Three typical sharp peaks common to fungal melanins were also found in *A. apis* melanin at 2920.2, 1631.5, and 1075.1 $cm^{-1}$, corresponding to the C–H group of quinone, C=C or C–C, and C=O and C–O of quinone neighboring the carboxyl group. Another stretching vibration at 2851 $cm^{-1}$ was attributed to the $–CH_2$ or $–CH_3$ group neighboring the quinone. The absorption at 2361 $cm^{-1}$ may indicate the stretching vibration of $–R_3NHX–$ (R=H or NH). Moreover, three medium-strong characteristic absorption peaks at 1737, 1631, and 1399 $cm^{-1}$ were attributed to the stretching vibrations of the aromatic skeleton, –COC–, and C=O groups, respectively. Overall, the molecular structure of *A. apis* melanin has fingerprint peaks of the common functional group characteristics of eumelanin, and contains a typical indole structure.

3.2.6 Raman spectroscopy

Raman spectroscopic analysis revealed that *A. apis* melanin showed three strong absorption bands at 1152, 1508, and 1005 $cm^{-1}$, attributed to the C=C and C–C stretching vibrations in aromatic compounds and the C–N stretching vibration of hydroxyl groups, respectively (Fig. 2). These three bands can be considered fingerprints specific to *A. apis* melanin. In addition, another band with minor intensity was observed in the range of 2824–2467 $cm^{-1}$, attributed to the C–H stretching vibration of lipid-based branching. Moreover, another signal peak was observed at 3497 $cm^{-1}$, which can be attributed to free radicals.

3.2.7 NMR analysis

$^1$H-NMR and $^{13}$C-NMR spectral analyses revealed that *A. apis* melanin has a series of broad absorption peaks, reflecting the complexity of the chemical structure and the characteristics of macromolecular compounds (Fig. 3). In the $^1$H-NMR spectrum (Fig. 3a), the HC=C resonance of the indole was observed at 7.1 ppm. The peaks with chemical shifts of 4.5–5.4 ppm indicated a C=C–H aromatic nucleus contained within the pigment structure. A $–CH_2$ might

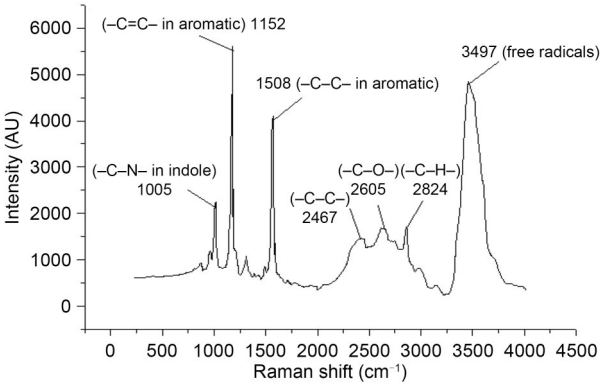


**Fig. 2 Raman spectrum of melanin from *Ascosphaera apis*. AU: arbitrary unit.**

cause the peaks between 3.1 and 4.2 ppm or a $–CH_3$ group connected to an N or O. The peaks between 2.2 and 2.5 ppm showed an NH group linked to the indole. The peaks between 0.8 and 1.5 ppm were caused by the $–CH_3$ group in $–CH_2CH_3$. In addition to the $^1$H-NMR spectrum, the $^{13}$C-NMR spectral analysis revealed that *A. apis* melanin has indole-based aromatic carbons and other long chains (Fig. 3b). The peaks at 63 and 204 ppm, between 76 and 101 ppm, and between 125 and 137 ppm were assigned to the carbon atoms of the CHO or $CH_2O$, carboxylic acid, and CH–N or CH–S group, respectively, in the indole aromatic structure. A resonance from the indole carbon skeleton appeared at 128 ppm, and a signal peak from a phenol structure at 136 ppm. However, the absence of resonances within the range of 10–40 ppm indicated no carbon atoms in methyl ($–CH_2CH_3$) or methylene ($–CH_2–$) group.

3.2.8 GC-MS analysis

Based on the quasi-molecular ion peaks of $[M]^+$ and $[M+H]^+$ at mass-to-charge ratio (*m*/*z*) 236.03 and 409.01, the molecular weight of *A. apis* melanin was determined to be 409 Da (Fig. S6). Combined with the results of elemental compound and chemical structure analysis (FTIR, $^1$H-NMR, $^{13}$C-NMR, and GC-MS), the molecular formula of *A. apis* melanin was speculated to be $C_{10}H_6O_4N_2$, and the possible chemical structure formula could be inferred (Fig. S7).

### 3.3 Biological activity of *A. apis* melanin

3.3.1 Antioxidant activity

The results of FRAP antioxidant analysis showed that compared with the ascorbic acid control, the

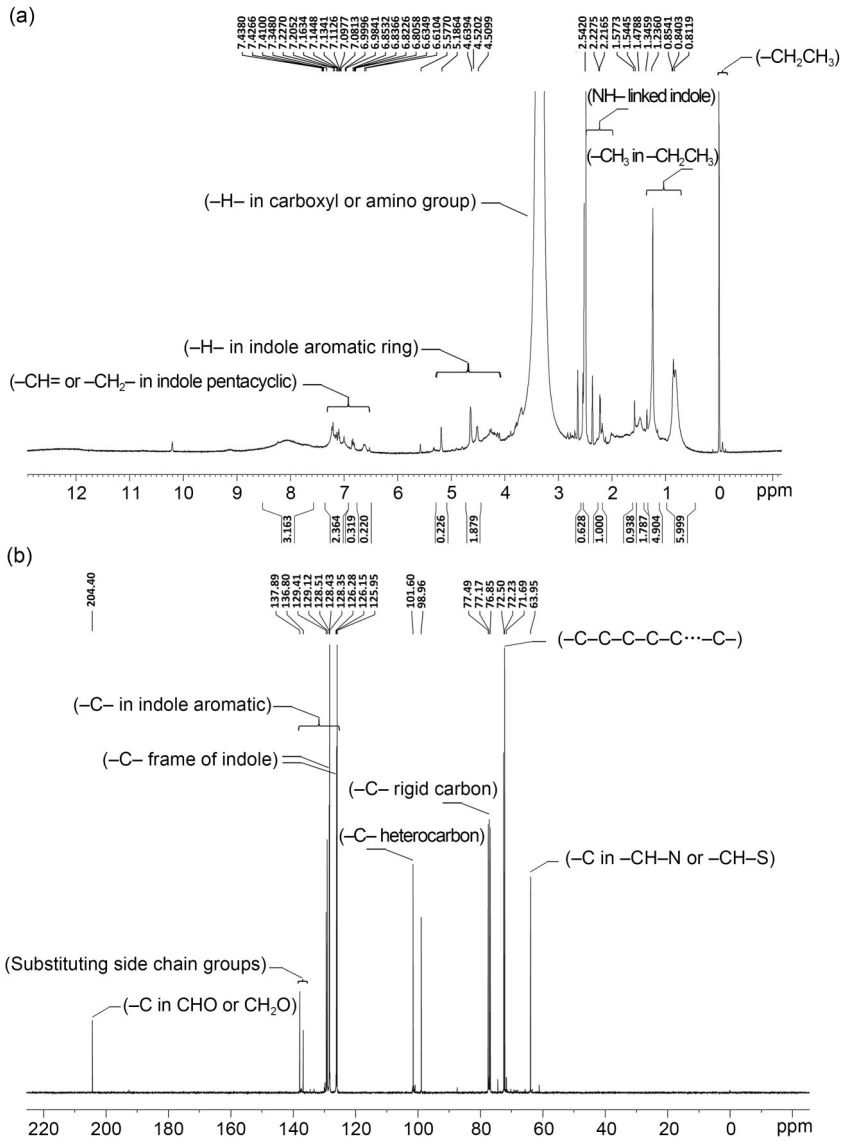


**Fig. 3 $^{1}$H-NMR (a) and $^{13}$C-NMR (b) spectra of melanin from *Ascosphaera apis*. NMR: nuclear magnetic resonance.**

antioxidant value of *A. apis* melanin increased with an increasing concentration of melanin (Fig. 4a) and exhibited a dose-dependent relationship ($Y$=0.2478$X$+0.07531, $R^2$=0.9981). When the pigment concentration was 5.0 mg/mL, the total antioxidant capacity of *A. apis* melanin was equivalent to the antioxidant capacity of 0.52 mmol/L ascorbic acid, and presented high total antioxidant activity.

### 3.3.2 Superoxide radical scavenging activity

The superoxide radical scavenging activity is considered a good indicator of the antioxidant activity of an extract. In this study, the superoxide radical scavenging activity of *A. apis* melanin increased with increasing concentration in a dose-dependent manner ($Y$=0.1029$X$+0.2193, $R^2$=0.9829) (Fig. 4b). At 5.0 mg/mL, the superoxide radical scavenging rates of *A. apis* melanin reached 71.2%. The $IC_{50}$ value of *A. apis* melanin was 26.23 mg/mL compared to the standard antioxidant ascorbic acid. These results indicated that *A. apis* melanin has a strong superoxide radical scavenging ability.

### 3.3.3 Hydroxyl radical scavenging activity

The hydroxyl radical scavenging activity was investigated at various concentrations (0–5.0 mg/mL) of *A. apis* melanin, and the results are shown in Fig. 4c. The hydroxyl radical scavenging activity of *A. apis*

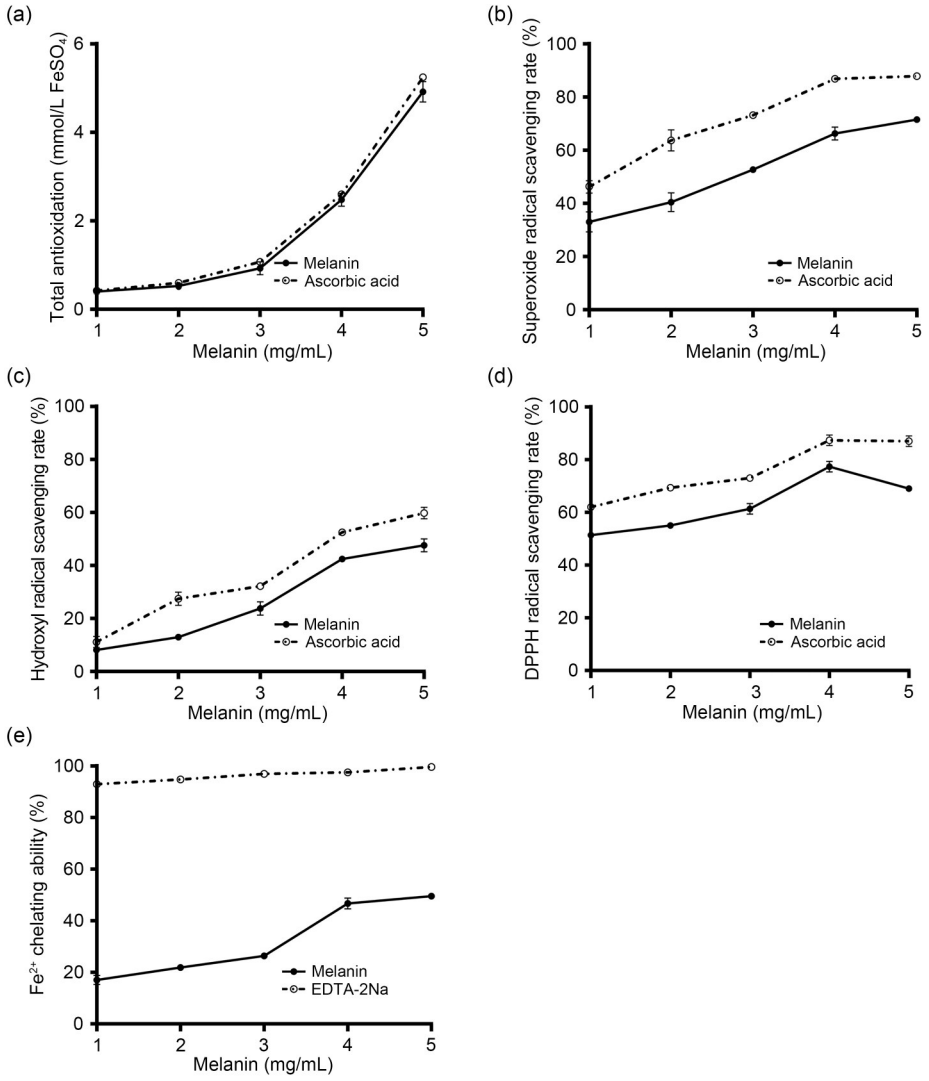


**Fig. 4 Antioxidant activity of melanin from *Ascosphaera apis*. (a) Ferric-reducing antioxidant power (FRAP) total antioxidant capacity; (b) Superoxide radical scavenging assay; (c) Hydroxyl radical scavenging assay; (d) 2,2-diphenyl-1-picrylhydrazyl (DPPH) radical scavenging assay; (e) Ferrous ion ($Fe^{2+}$) chelating assay. EDTA-2Na: ethylenediaminetetraacetic acid disodium salt.**

melanin increased with increasing concentration, exhibited a dose-effect relationship ($Y$=0.1086$X$−0.05596, $R^2$=0.9582), and showed good hydroxyl radical scavenging activity with an $IC_{50}$ value of 5.467 mg/mL and good scavenging rates (47.1%) at a concentration of 5.0 mg/mL (Fig. 4c). These results demonstrated that *A. apis* melanin has a strong free radical scavenging ability.

### 3.3.4 DPPH radical scavenging activity

The radical scavenging activity of *A. apis* melanin against stable DPPH was determined spectrophotometrically. The results indicated that the DPPH scavenging activity of *A. apis* melanin increased with increasing concentration and showed significant radical scavenging activity with an $IC_{50}$ value of 74.49 mg/mL (Fig. 4d). When the pigment concentration was 4 mg/mL, the DPPH scavenging rate of *A. apis* melanin reached 69.3%, slightly lower than that of ascorbic acid (87.2%). These results indicated that *A. apis* melanin has a notable effect on DPPH radical scavenging activity.

### 3.3.5 Chelating effect on ferrous ions

The ability of *A. apis* pigment to bind ferric ions increased with increasing concentration in a dose-dependent manner (Fig. 4e). The $IC_{50}$ value of *A. apis* melanin was 58.79 mg/mL compared to 0.83 mg/mL

ethylenediaminetetraacetic acid disodium salt (EDTA-2Na). At 5 mg/mL, the $Fe^{2+}$ chelating rate of *A. apis* melanin was 49.6%. These results suggested that *A. apis* melanin has significant chelating activity against $Fe^{2+}$.

### 3.4 Subcellular localization characteristics of *A. apis* melanin

SEM, TEM, and IFA were performed to determine the precise location of melanin in the *A. apis* spores. The pigment extracted by enzymatic hydrolysis formed granules of the polymer. The granules retained the spherical shape of the spores as viewed with the electron microscope (Fig. S8), and represented the melanin "ghost." Under SEM, the *A. apis* melanin ghost had an average size of 2 μm×1 μm, consistent with that of normal spores in this study (Figs. S8a and S8b) and our previous study (Li Z et al., 2018). The most striking feature of the melanin ghosts was their concavity. They appeared to be empty shells that had lost the endoplasm (Fig. S8b). However, the surface of the pigment ghosts was not as smooth as that of normal wild-type spores (Figs. S8a and S8b). TEM showed that the melanin granular particles were clustered and formed two electron-dense layers, filling the endospore (about 20 nm thick) and exospore (about 50 nm thick) of the normal spore (Figs. S8c and S8e). However, the pigment of the ghosts appeared to be more concave, flatter, and smaller (about 1.5 μm×0.5 μm) than that of normal spores (about 2.0 μm×1.0 μm) (Figs. S8d and S8f). In addition, the surface of the ghosts was covered with granular particles that were 50–300 nm thick, and looser than that of the melanin distributed on the normal spores (Figs. S8c and S8d). The IFA showed that the spore coat displayed a bright green fluorescence signal (Fig. 5) after incubation with the *A. apis* melanin antiserum, while no such signal was observed in the negative control. The results suggested that melanin was localized on the spore wall of *A. apis*.

### 3.5 No apparent toxic effects of melanin-deficient spores on bee

Spores with functionally defective melanin were successfully prepared by inhibiting melanin synthesis with tricyclazole (Fig. 6a) or incubating spores with melanin antibody (Fig. 6b). Then, the defective spores were fed to bee larvae for infection experiments. Survival analysis showed that the mortality of bee larvae fed spores without melanin as a result of tricyclazole inhibition or incubation with melanin antibody was not significantly different from that of the normal spore infection group (Fig. 6c). The results showed that this melanin-deficient spore was still pathogenic to bee larvae, indicating that melanin did not affect the virulence of *A. apis* spores-infecting bees.

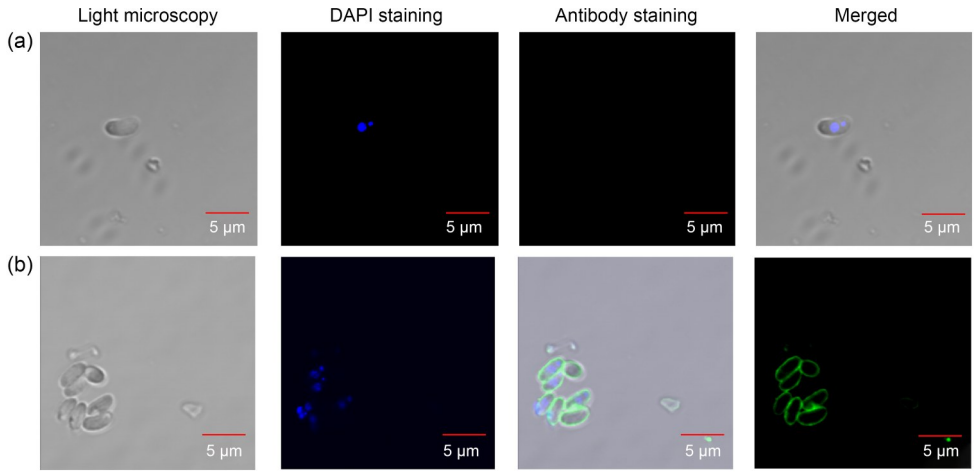


**Fig. 5 Indirect immunofluorescence assay (IFA) of the subcellular localization of melanin from *Ascosphaera apis*. Purified spores were visualized with a fluorescence microscope after incubation with primary antibodies against melanin produced from *A. apis*. (a) Negative control. No green fluorescence signals were detected in samples pretreated with negative serum. (b) Melanin antiserum treatment. Blue and green fluorescence signals were observed in samples treated with 4',6-diamidino-2-phenylindole (DAPI) and melanin antiserum. The anti-melanin serum was diluted to 1:100 (volume ratio). The secondary antibody was fluorescein isothiocyanate (FITC)-conjugated goat anti-mouse immunoglobulin G (IgG; Sigma) at a 1:64 (volume ratio) dilution.**

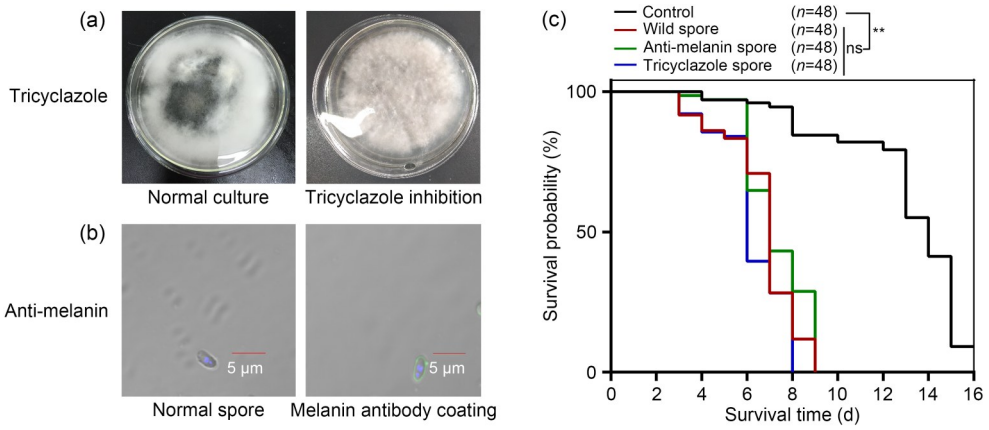


**Fig. 6 Role of melanin in virulence of *Ascosphaera apis* spore infection. (a) *A. apis* spores incubated with melanin antibody. (b) *A. apis* spores without melanin following culture with tricyclazole. (c) The survival rate of honey bee *A. mellifera* larvae was monitored for 16 d following feeding with *A. apis* spores ($1\times10^5$ spores/bee). The control group consisted of bee larvae fed artificial food (mass fraction: 50% royal jelly, 6% fructose, 6% glucose, 2% yeast extract, and 36% dd$H_2O$). The wild spore group consisted of bee larvae fed wild-type *A. apis* spores. The anti-melanin spore group consisted of bee larvae fed *A. apis* spores incubated with melanin antibody. The tricyclazole spore group consisted of bee larvae fed *A. apis* spores without melanin following culture with tricyclazole. Statistical significance was set at $^{**}$ $P<0.01$ (Kaplan-Meier survival analysis, log-rank test for overall comparison). ns: not significant.**

## 4 Discussion

Melanins are divided into three main types: eumelanin, phaeomelanin, and allomelanin. Eumelanin is a brown or black nitrogen-containing heterogeneous macromolecular compound derived from 5,6-dihydroxyindole-2-carboxylic acid (DHICA) and 5,6-dihydroxyindole (DHI). DHICA and DHI are derived from DOPA and DOPA quinone (Tadokoro et al., 2003; Sansinenea and Ortiz, 2015). Some of the key physicochemical properties and chemical structures of eumelanin have been clearly defined and are used as the standard for melanin identification: (1) melanin is insoluble in acidic solutions and common organic reagents (Butler and Day, 1998); (2) melanin has a 6%–11% N content, low S content, and a low molar ratio of S/N in elemental composition (Tu et al., 2009; Sun et al., 2016a, 2016b; Huang et al., 2018); (3) melanin is a macromolecule of DHI and DHICA, which is primarily formed from catechol monomers, and especially contains an indole in its chemical structure (Meredith and Sarna, 2006). Melanin is a complex mixture that is difficult to separate into monomers. Therefore, multiple analytical techniques need to be combined to confirm its identification. Melanin contains a unique and stable population of organic free radical compounds (Enochs et al., 1993; Prados-Rosales et al., 2015), resulting in characteristic EPR behavior and inducing a unique signal peak near 3500 G in the EPR spectrum (Suwannarach et al., 2019). EPR spectroscopy is thus considered the most reliable technique for distinguishing the characteristics of melanins (Enochs et al., 1993). In this study, we successfully extracted dark-colored pigments produced by *A. apis* using alkali extraction, acid hydrolysis, and repeated precipitation. Its chemical structure was comprehensively characterized by combining UV, elemental composition, FTIR, Raman spectroscopy, NMR, EPR, and GC-MS techniques. First, we showed that the *A. apis* pigment is insoluble in common organic solvents and precipitates in HCl (Fig. S2), consistent with the typical solubility characteristics of eumelanin (Gómez and Nosanchuk, 2003). Second, we found that the *A. apis* pigment has elemental composition characteristics similar to those of eumelanin from *Streptomyces* sp. (Li C et al., 2018), especially the low S content (mass fraction: 0.86%) and low S/N ratio (0.13) (Fig. S4). Third, through FTIR and NMR analyses, we showed that the *A. apis* pigment has a typical indole structure. The characteristic absorption of the indole structure occurred at 2361 $cm^{-1}$ and 804–572 $cm^{-1}$ in the FTIR spectrum (Figs. S5 and 3). The CH=C resonance of the indole appeared at 7.1 ppm in the $^{1}$H-NMR spectrum. In the $^{13}$C-NMR spectrum, signal peaks from the indole-based

aromatic carbons appeared from 125 to 137 ppm. In addition, a resonance from the indole carbon skeleton appeared at 128 ppm, and no signal peak from a phenol structure was observed at 136 ppm. In addition, two typical eumelanin signature C=C and C–C groups were present in the aromatic indole structure (Fig. 2), thus proving that there is an indole moiety in the *A. apis* pigment. Combined with GC-MS data, this showed that the phenyl and pentacyclic rings linked to the indole group reported in most melanin structures were replaced by carboxyl, amino, and ester groups in the *A. apis* pigment (Fig. S6). Fourth, and most importantly, a stable free radical compound (generating a signal at 3510 G in the EPR spectrum; Fig. 1) reported in most fungal melanin structures (Morris-Jones et al., 2003; Nosanchuk and Casadevall, 2003; al Khatib et al., 2018; Camacho et al., 2019), which is considered a unique feature of melanin, was also found in the *A. apis* pigment. By comparing the solubility characteristics, elemental composition, chemical structure, and functional groups of the typical melanins reported above, the *A. apis* pigment in this study was identified as a DOPA-eumelanin.

The location of melanin in cells determines its corresponding biological functions and has thus received widespread attention. Some fungal melanins have been found to be part of the spore wall or spore extracellular matrices. For instance, melanins of *C. neoformans* are arranged neatly and bridged to each other through chitin or polysaccharides, forming an electron-dense layer from the cell wall to the plasma membrane (Nosanchuk and Casadevall, 2003). Functional studies have shown that this type of melanin is generally involved in the virulence of invasion and protection against oxidant stress, ionizing radiation, and antifungal drugs (Dixon et al., 1989; Nosanchuk and Casadevall, 2003; Hernández-Chávez et al., 2017). In addition, cell wall melanization can also increase the mechanical strength and rigidity of cells, changing cell permeability and turgor forces (Money et al., 1998). In contrast, melanin in *Candida* is externalized from spores in the form of electron-dense melanosomes that are free or usually loosely bound to the outside of the cell wall, and which cannot form an electron-dense layer to protect the spores (Walker et al., 2010). There are also a few species of melanin located in special vacuoles or intracellular vesicles, functioning as “virulence bags” or involved in cell autolysis (Rodrigues et al., 2008; Smith and Casadevall, 2019). Our previous study found that the spore wall consists of an electron-dense outer surface layer (exospore), an electron-lucent layer, and an electron-dense inner plasma membrane. The exospore and endospore together form a spore coat with a uniform thickness that helps spores resist various environmental pressures (Li Z et al., 2018). In this study, the spore wall was observed with SEM and TEM. The results showed that *A. apis* melanin clustered to form an electron-dense layer extending throughout the entire cell wall in immature and mature spores (Figs. S8 and 5). Therefore, *A. apis* melanin probably has similar functions to the melanins mentioned above in fungal species. Moreover, considering that in the invasion process, the *A. apis* mycelium can overcome the gut wall barrier and eventually penetrate the entire honeybee larva, melanin located within the spore wall is likely similar to the melanin of *Gaeumannomyces graminis* var. *graminis* (Money et al., 1998), which can promote spores to generate enormous turgor pressures and provide the necessary force to enable penetration by spore mycelia. *A. apis* melanin within the cell wall probably also helps spores survive in drought or high osmotic pressure environments, resulting in *A. apis* being able to survive and remain infectious, even in beehives that have been unused and contain mummified larvae that have been dead for a long time.

Antioxidant capacities refer to DPPH radical scavenging, superoxide radical scavenging, hydroxyl radical scavenging, nitric oxide scavenging, reducing power and metal chelating abilities. These antioxidant capacities are the basic functions and characteristics of almost all reported melanins and have become an important index of melanin identification. Melanins from *Lachnum* YM-346 (Ye et al., 2012), *Actinoalloteichus* sp. (Manivasagan et al., 2013), *Schizophyllum commune* (Arun et al., 2015), *Streptomyces* sp. (Arun et al., 2015), and *Actinomycetes* sp. (Manivasagan et al., 2013) have strong antioxidant activity, which is helpful in protecting cells from oxidative damage caused by various stresses inside and outside cells. In this study, FRAP, DPPH, superoxide and hydroxyl radical scavenging analyses showed that *A. apis* melanin also has a strong antioxidant capacity (Fig. 4). The antioxidant ability is probably helpful for enabling *A. apis* spores to survive in harsh environments.

Melanin can also bind directly with metal ions such as $Fe^{2+}$, exhibiting a high affinity and high capacity (Guo et al., 2010; Li et al., 2016). This is because the aromatic components and functional groups in melanin, such as hydroxyl, carboxyl, amine, and phenol groups, provide a chemical basis for the interaction of melanin with many organic and inorganic molecules (Solano, 2017). For example, $Mg^{2+}$, $Ca^{2+}$, and $Zn^{2+}$ preferentially bind to the carboxyl group (Fan et al., 2014), $Cu^{2+}$ binds to the hydroxyl group (Samokhvalov et al., 2004), and $Fe^{2+}$ prefers to coordinate with hydroxyl groups, amines, imines, and acetate groups (Hong and Simon, 2007) of melanin. In this study, the FTIR and Raman data indicated that *A. apis* melanin has amino, hydroxyl, carboxyl, and other potential fatty side chain groups (Figs. S5 and 2). Therefore, *A. apis* melanin can also chelate to iron due to the presence of these high-affinity groups. The FRAP antioxidant activity analysis showed that *A. apis* melanin could bind to $Fe^{3+}$ and reduce $Fe^{3+}$ to $Fe^{2+}$ (Fig. 4). Many studies have confirmed that metal elements such as iron play an important role in the metabolism of cells (Aisen et al., 2001; Recalcati et al., 2010; Geissler and Singh, 2011). Obtaining iron and other metal elements from the environment is an important strategy for multicellular or single-cell microorganisms (Sargent et al., 2005). For *A. apis*, melanin can chelate iron and potentially bind other metals, providing a good tool for spores to absorb essential metal elements from host bees and other environments.

Fungal melanin usually contributes to spore pathogenicity and survival in their host. For example, *A. fumigatus* melanin can inhibit nicotinamide adenine dinucleotide phosphate (NADPH) oxidase-dependent LC3-associated phagocytosis (LAP) activation in phagocytes, thus protecting spores from being engulfed by host phagocytes (Akoumianaki et al., 2016). *C. neoformans* melanin can transfer or store electrons to alter the fungal cell surface charge, thus interfering with the transfer of the host electron transfer chain, which may contribute to inhibiting phagocytosis by the host (Wang et al., 1995; Nosanchuk and Casadevall, 1997). The ability of melanin to enhance pathogenicity is also commonly found in other fungi, such as *Sporothrix schenckii* (Romero-Martinez et al., 2000), *Fonsecaea pedrosoi* (Cunha et al., 2005), and *Exophiala* spp. (Peltroche-Llacsahuanga et al., 2003). This ability of fungal melanin rests on two major premises, spore wall localization and the ability to be a highly effective scavenger of free radicals, which are consistent with the results in this paper. Therefore, *A. apis* melanin could also contribute to the pathogenicity of spores. However, the survival rate of the larvae did not increase significantly after using melanin-deficient spores (Fig. 6) to infect bee larvae. This result indicated that *A. apis* melanin did not promote the pathogenicity of spores. Nonetheless, we cannot rule out the possibility that *A. apis*, similar to *A. fumigatus*, uses the redox functions of melanin to interfere with the host's life activities (Akoumianaki et al., 2016) or that *C. neoformans* uses melanin to interfere with the host's electron transfer (Wang et al., 1995). These effects promoting infection probably affect only the metabolism of the host rather than its survival. This possibility needs further analysis by transcriptomics and metabolomics.

Note that this study investigated only melanin produced from spores, whereas previous studies normally used mycelium cultures to prepare melanin. *A. apis* sporangiophores, sporophores or sporocysts, and spores contain melanin. The location of melanin in organisms usually determines its corresponding biological function. Melanin from the other three sources is likely to differ in its chemical structure, physicochemical properties, and biological activity. Therefore, future research should compare these three melanins to provide a more comprehensive understanding of fungal melanins.

## 5 Conclusions

This paper is the first report on melanin produced by *A. apis*. *A. apis* melanin is a eumelanin with a typical indole structure. It is located on the spore wall, has strong antioxidant activity, can potentially chelate to metal ions, and does not enhance the virulence of *A. apis* spores. This work provides valuable information for understanding the architecture and function of melanin in pathogenic fungi. Future studies will focus on the functional analysis of melanin in *A. apis* in relation to resistance to environmental stresses.

**Acknowledgments**

This work was supported by the Science and Technology Project of the Chongqing Municipal Education Commission (No. KJZD-K202100502), the Natural Science Foundation Project of Chongqing (No. cstc2021jcyj-msxmX0422), the

Higher Education Teaching Reform Research Project of the Chongqing Municipal Education Commission (Nos. 213132 and KJ173061), the Postgraduate Education and Teaching Reform Research Project of Chongqing Normal University (No. xyjg21012), the Creation & Research Team in College and Universities of Chongqing Municipal Education Commission (No. CXQT21013), the College Student Innovation and Entrepreneurship Training Program Project of the Chongqing Municipal Education Commission (No. 202110637013), and the Natural Science Foundation Project of Chongqing Normal University (No. 13XLB009), China.

## Author contributions

Zhi LI and Zeyang ZHOU conceived the research and designed experiments. Zhi LI, Hui HENG, and Qiqian QIN performed the experiments and analysis. Zhi LI, Hui HENG, Lanchun CHEN, and Yuedi WANG interpreted the data and wrote the paper. All authors have read and approved the final manuscript, and therefore, have full access to all the data in the study and take responsibility for the integrity and security of the data.

## Compliance with ethics guidelines

Zhi LI, Hui HENG, Qiqian QIN, Lanchun CHEN, Yuedi WANG, and Zeyang ZHOU declare that they have no conflict of interest.

The animal experimental processes were approved by the Ethnic Committee of College of Life Sciences, Chongqing Normal University and conducted in strict accordance with the standard of the Guide for the Care and Use of Laboratory Animals published by the Ministry of Science and Technology of the People's Republic of China in 2006.

## References

Aisen P, Enns C, Wessling-Resnick M, 2001. Chemistry and biology of eukaryotic iron metabolism. *Int J Biochem Cell Biol*, 33(10):940-959. https://doi.org/10.1016/S1357-2725(01)00063-2

Akoumianaki T, Kyrmizi I, Valsecchi I, et al., 2016. *Aspergillus* cell wall melanin blocks LC3-associated phagocytosis to promote pathogenicity. *Cell Host Microbe*, 19(1):79-90. https://doi.org/10.1016/j.chom.2015.12.002

al Khatib M, Harir M, Costa J, et al., 2018. Spectroscopic characterization of natural melanin from a *Streptomyces cyaneofuscatus* strain and comparison with melanin enzymatically synthesized by tyrosinase and laccase. *Molecules*, 23(8):1916. https://doi.org/10.3390/molecules23081916

Aronstein KA, Murray KD, 2010. Chalkbrood disease in honey bees. *J Invertebr Pathol*, 103(S1):S20-S29. https://doi.org/10.1016/j.jip.2009.06.018

Arun G, Eyini M, Gunasekaran P, 2015. Characterization and biological activities of extracellular melanin produced by *Schizophyllum commune* (Fries). *Indian J Exp Biol*, 53(6):380-387.

Bailey L, 1968. Honey bee pathology. *Annu Rev Entomol*, 13: 191-212. https://doi.org/10.1146/annurev.en.13.010168.001203

Bao T, Zhang M, Zhou YQ, et al., 2021. Phenolic profile of jujube fruit subjected to gut microbiota fermentation and its antioxidant potential against ethyl carbamate-induced oxidative damage. *J Zhejiang Univ-Sci B (Biomed & Biotechnol)*, 22(5):397-409. https://doi.org/10.1631/jzus.B2000754

Bersuder P, Hole M, Smith G, 1998. Antioxidants from a heated histidine-glucose model system. I: Investigation of the antioxidant role of histidine and isolation of antioxidants by high-performance liquid chromatography. *J Am Oil Chem Soc*, 75(2):181-187. https://doi.org/10.1007/s11746-998-0030-y

Butler MJ, Day AW, 1998. Fungal melanins: a review. *Can J Microbiol*, 44(12):1115-1136. https://doi.org/10.1139/w98-119

Camacho E, Vij R, Chrissian C, et al., 2019. The structural unit of melanin in the cell wall of the fungal pathogen *Cryptococcus neoformans*. *J Biol Chem*, 294(27):10471-10489. https://doi.org/10.1074/jbc.RA119.008684

Césarini JP, 1990. Hair melanin and hair color. *In*: Orfanos CE, Happle R (Eds.), Hair and Hair Diseases. Springer, Berlin, Heidelberg, p.165-197. https://doi.org/10.1007/978-3-642-74612-3_8

Chen YG, Shen ZJ, Chen XP, 2009. Evaluation of free radicals scavenging and immunity-modulatory activities of Purslane polysaccharides. *Int J Biol Macromol*, 45(5): 448-452. https://doi.org/10.1016/j.ijbiomac.2009.07.009

Cunha MML, Franzen AJ, Alviano DS, et al., 2005. Inhibition of melanin synthesis pathway by tricyclazole increases susceptibility of *Fonsecaea pedrosoi* against mouse macrophages. *Microsc Res Tech*, 68(6):377-384. https://doi.org/10.1002/jemt.20260

Dadachova E, Bryan RA, Huang XC, et al., 2007. Ionizing radiation changes the electronic properties of melanin and enhances the growth of melanized fungi. *PLoS ONE*, 2(5):e457. https://doi.org/10.1371/journal.pone.0000457

de la Rosa JM, Martin-Sanchez PM, Sanchez-Cortes S, et al., 2017. Structure of melanins from the fungi *Ochroconis lascauxensis* and *Ochroconis anomala* contaminating rock art in the Lascaux Cave. *Sci Rep*, 7:13441. https://doi.org/10.1038/s41598-017-13862-7

Dixon DM, Polak A, Conner GW, 1989. Mel$^-$ mutants of *Wangiella dermatitidis* in mice: evaluation of multiple mouse and fungal strains. *J Med Vet Mycol*, 27(5):335-341. https://doi.org/10.1080/02681218980000451

Enochs WS, Nilges MJ, Swartz HM, 1993. A standardized test for the identification and characterization of melanins using electron paramagnetic resonance (EPR) spectroscopy. *Pigment Cell Res*, 6(2):91-99. https://doi.org/10.1111/j.1600-0749.1993.tb00587.x

Fan QL, Cheng K, Hu X, et al., 2014. Transferring biomarker into molecular probe: melanin nanoparticle as a naturally active platform for multimodality imaging. *J Am Chem*

*Soc*, 136(43):15185-15194. https://doi.org/10.1021/ja505412p

Fiore G, Poli A, di Cosmo A, et al., 2004. Dopamine in the ink defence system of *Sepia officinalis*: biosynthesis, vesicular compartmentation in mature ink gland cells, nitric oxide (NO)/cGMP-induced depletion and fate in secreted ink. *Biochem J*, 378(3):785-791. https://doi.org/10.1042/BJ20031864

Fogarty RV, Tobin JM, 1996. Fungal melanins and their interactions with metals. *Enzyme Microb Technol*, 19(4):311-317. https://doi.org/10.1016/0141-0229(96)00002-6

Galván I, Araujo-Andrade C, Marro M, et al., 2018. Raman spectroscopy quantification of eumelanin subunits in natural unaltered pigments. *Pigment Cell Melanoma Res*, 31(6):673-682. https://doi.org/10.1111/pcmr.12707

Geissler C, Singh M, 2011. Iron, meat and health. *Nutrients*, 3(3):283-316. https://doi.org/10.3390/nu3030283

Gómez BL, Nosanchuk JD, 2003. Melanin and fungi. *Curr Opin Infect Dis*, 16(2):91-96. https://doi.org/10.1097/00001432-200304000-00005

Gómez BL, Nosanchuk JD, Díez S, et al., 2001. Detection of melanin-like pigments in the dimorphic fungal pathogen *Paracoccidioides brasiliensis* in vitro and during infection. *Infect Immun*, 69(9):5760-5767. https://doi.org/10.1128/iai.69.9.5760-5767.2001

Guo T, Hou CL, Wei L, et al., 2010. Antioxidant activities of extracts and sub-fractions from *Tuber indicum*. *Mycosystema*, 29(4):569-575 (in Chinese). https://doi.org/10.13346/j.mycosystema.2010.04.025

Guo X, Chen SG, Hu YQ, et al., 2014. Preparation of water-soluble melanin from squid ink using ultrasound-assisted degradation and its anti-oxidant activity. *J Food Sci Technol*, 51(12):3680-3690. https://doi.org/10.1007/s13197-013-0937-7

Heath L, Gaze BM, 1987. Carbon dioxide activation of spores of the chalkbrood fungus *Ascosphaera apis*. *J Apicult Res*, 26(4):243-246. https://doi.org/10.1080/00218839.1987.11100768

Hernández-Chávez MJ, Pérez-García LA, Niño-Vega GA, et al., 2017. Fungal strategies to evade the host immune recognition. *J Fungi*, 3(4):51. https://doi.org/10.3390/jof3040051

Hill HZ, 1991. Melanins in the photobiology of skin cancer and the radiobiology of melanomas. *In*: Wilson SH (Ed.), Cancer Biology and Biosynthesis. Telford Press, Caldwell, p.31-53.

Hong L, Simon JD, 2007. Current understanding of the binding sites, capacity, affinity, and biological significance of metals in melanin. *J Phys Chem B*, 111(28):7938-7947. https://doi.org/10.1021/jp071439h

Huang L, Liu MY, Huang HY, et al., 2018. Recent advances and progress on melanin-like materials and their biomedical applications. *Biomacromolecules*, 19(6):1858-1868. https://doi.org/10.1021/acs.biomac.8b00437

Jacobson ES, 2000. Pathogenic roles for fungal melanins. *Clin Microbiol Rev*, 13(4):708-717. https://doi.org/10.1128/CMR.13.4.708

Kim YJ, Wu W, Chun SE, et al., 2013. Biologically derived melanin electrodes in aqueous sodium-ion energy storage devices. *Proc Natl Acad Sci USA*, 110(52):20912-20917. https://doi.org/10.1073/pnas.1314345110

Kwon-Chung K, Polacheck I, Popkin TJ, 1982. Melanin-lacking mutants of *Cryptococcus neoformans* and their virulence for mice. *J Bacteriol*, 150(3):1414-1421. https://doi.org/10.1128/jb.150.3.1414-1421.1982

Langfelder K, Streibel M, Jahn B, et al., 2003. Biosynthesis of fungal melanins and their importance for human pathogenic fungi. *Fungal Genet Biol*, 38(2):143-158. https://doi.org/10.1016/s1087-1845(02)00526-1

Li C, Ji CM, Tang BP, 2018. Purification, characterisation and biological activity of melanin from *Streptomyces* sp. *FEMS Microbiol Lett*, 365(19):fny077. https://doi.org/10.1093/femsle/fny077

Li YW, Xie YJ, Wang Z, et al., 2016. Structure and function of iron-loaded synthetic melanin. *ACS Nano*, 10(11):10186-10194. https://doi.org/10.1021/acsnano.6b05502

Li Z, Pan GQ, Li T, et al., 2012. SWP5, a spore wall protein, interacts with polar tube proteins in the parasitic microsporidian *Nosema bombycis*. *Eukaryot Cell*, 11(2):229-237. https://doi.org/10.1128/EC.05127-11

Li Z, You XL, Wang LL, et al., 2018. Spore morphology and ultrastructure of an *Ascosphaera apis* strain from the honeybees (*Apis mellifera*) in southwest China. *Mycologia*, 110(2):325-338. https://doi.org/10.1080/00275514.2018.1442084

Liu QM, Xiao JJ, Liu BT, et al., 2018. Study on the preparation and chemical structure characterization of melanin from *Boletus griseus*. *Int J Mol Sci*, 19(12):3736. https://doi.org/10.3390/ijms19123736

Manivasagan P, Venkatesan J, Senthilkumar K, et al., 2013. Isolation and characterization of biologically active melanin from *Actinoalloteichus* sp. MA-32. *Int J Biol Macromol*, 58:263-274. https://doi.org/10.1016/j.ijbiomac.2013.04.041

McGraw KJ, Safran RJ, Wakamatsu K, 2005. How feather colour reflects its melanin content. *Funct Ecol*, 19(5):816-821. https://doi.org/10.1111/j.1365-2435.2005.01032.x

Menon IA, Persad S, Haberman HF, et al., 1983. A comparative study of the physical and chemical properties of melanins isolated from human black and red hair. *J Invest Dermatol*, 80(3):202-206. https://doi.org/10.1111/1523-1747.ep12534045

Meredith P, Sarna T, 2006. The physical and chemical properties of eumelanin. *Pigment Cell Res*, 19(6):572-594. https://doi.org/10.1111/j.1600-0749.2006.00345.x

Money NP, Caesar-TonThat T, Frederick B, et al., 1998. Melanin synthesis is associated with changes in hyphopodial turgor, permeability, and wall rigidity in *Gaeumannomyces graminis* var. *graminis*. *Fungal Genet Biol*, 24(1-2):240-251. https://doi.org/10.1006/fgbi.1998.1052

Montefiori DC, Zhou JY, 1991. Selective antiviral activity of synthetic soluble L-tyrosine and L-dopa melanins against

human immunodeficiency virus in vitro. *Antiviral Res*, 15(1):11-25. https://doi.org/10.1016/0166-3542(91)90037-r

Morris-Jones R, Youngchim S, Gomez BL, et al., 2003. Synthesis of melanin-like pigments by *Sporothrix schenckii* in vitro and during mammalian infection. *Infect Immun*, 71(7):4026-4033. https://doi.org/10.1128/IAI.71.7.4026-4033.2003

Morse RA, 1978. Honey Bee Pests, Predators, and Diseases. Comstock Publishing Associates, Division of Cornell University Press, Ithaca and London, p.430.

Nappi AJ, Christensen BM, 2005. Melanogenesis and associated cytotoxic reactions: applications to insect innate immunity. *Insect Biochem Mol Biol*, 35(5):443-459. https://doi.org/10.1016/j.ibmb.2005.01.014

Nosanchuk JD, Casadevall A, 1997. Cellular charge of *Cryptococcus neoformans*: contributions from the capsular polysaccharide, melanin, and monoclonal antibody binding. *Infect Immun*, 65(5):1836-1841. https://doi.org/10.1128/iai.65.5.1836-1841.1997

Nosanchuk JD, Casadevall A, 2003. The contribution of melanin to microbial pathogenesis. *Cell Microbiol*, 5(4):203-223. https://doi.org/10.1046/j.1462-5814.2003.00268.x

Nosanchuk JD, Casadevall A, 2006. Impact of melanin on microbial virulence and clinical resistance to antimicrobial compounds. *Antimicrob Agents Chemother*, 50(11): 3519-3528. https://doi.org/10.1128/AAC.00545-06

Nosanchuk JD, Stark RE, Casadevall A, 2015. Fungal melanin: what do we know about structure? *Front Microbiol*, 6: 1463. https://doi.org/10.3389/fmicb.2015.01463

Peltroche-Llacsahuanga H, Schnitzler N, Jentsch S, et al., 2003. Analyses of phagocytosis, evoked oxidative burst, and killing of black yeasts by human neutrophils: a tool for estimating their pathogenicity? *Med Mycol*, 41(1):7-14. https://doi.org/10.1080/mmy.41.1.7.14

Prados-Rosales R, Toriola S, Nakouzi A, et al., 2015. Structural characterization of melanin pigments from commercial preparations of the edible mushroom *Auricularia auricula*. *J Agric Food Chem*, 63(33):7326-7332. https://doi.org/10.1021/acs.jafc.5b02713

Raman NM, Ramasamy S, 2017. Genetic validation and spectroscopic detailing of DHN-melanin extracted from an environmental fungus. *Biochem Biophys Rep*, 12:98-107. https://doi.org/10.1016/j.bbrep.2017.08.008

Recalcati S, Minotti G, Cairo G, 2010. Iron regulatory proteins: from molecular mechanisms to drug development. *Antioxid Redox Signal*, 13(10):1593-1616. https://doi.org/10.1089/ars.2009.2983

Richman A, Kafatos FC, 1996. Immunity to eukaryotic parasites in vector insects. *Curr Opin Immunol*, 8(1):14-19. https://doi.org/10.1016/s0952-7915(96)80099-9

Rodrigues ML, Nimrichter L, Oliveira DL, et al., 2008. Vesicular trans-cell wall transport in fungi: a mechanism for the delivery of virulence-associated macromolecules? *Lipid Insights*, 2:27-40. https://doi.org/10.4137/lpi.s1000

Romero-Martinez R, Wheeler M, Guerrero-Plata A, et al., 2000. Biosynthesis and functions of melanin in *Sporothrix schenckii*. *Infect Immun*, 68(6):3696-3703. https://doi.org/10.1128/IAI.68.6.3696-3703.2000

Samokhvalov A, Liu Y, Simon JD, 2004. Characterization of the Fe(III)-binding site in *Sepia* eumelanin by resonance Raman confocal microspectroscopy. *Photochem Photobiol*, 80(1):84-88. https://doi.org/10.1111/j.1751-1097.2004.tb00053.x

Sansinenea E, Ortiz A, 2015. Melanin: a photoprotection for *Bacillus thuringiensis* based biopesticides. *Biotechnol Lett*, 37(3):483-490. https://doi.org/10.1007/s10529-014-1726-8

Sargent PJ, Farnaud S, Evans RW, 2005. Structure/function overview of proteins involved in iron storage and transport. *Curr Med Chem*, 12(23):2683-2693. https://doi.org/10.2174/092986705774462969

Schweitzer AD, Howell RC, Jiang ZW, et al., 2009. Physicochemical evaluation of rationally designed melanins as novel nature-inspired radioprotectors. *PLoS ONE*, 4(9): e7229. https://doi.org/10.1371/journal.pone.0007229

Smith DFQ, Casadevall A, 2019. The role of melanin in fungal pathogenesis for animal hosts. *Curr Top Microbiol Immunol*, 422:1-30. https://doi.org/10.1007/82_2019_173

Solano F, 2017. Melanin and melanin-related polymers as materials with biomedical and biotechnological applications—cuttlefish ink and mussel foot proteins as inspired biomolecules. *Int J Mol Sci*, 18(7):1561. https://doi.org/10.3390/ijms18071561

Spiltoir CF, 1955. Life cycle of *Ascosphaera apis* (*Pericystis apis*). *Am J Bot*, 42(6):501-508. https://doi.org/10.1002/j.1537-2197.1955.tb11154.x

Spiltoir CF, Olive LS, 1955. A reclassification of the genus *Pericystis* Betts. *Mycologia*, 47(2):238-244. https://doi.org/10.2307/3755414

Sun SJ, Zhang XJ, Sun SW, et al., 2016a. Production of natural melanin by *Auricularia auricula* and study on its molecular structure. *Food Chem*, 190:801-807. https://doi.org/10.1016/j.foodchem.2015.06.042

Sun SJ, Zhang XJ, Chen WX, et al., 2016b. Production of natural edible melanin by *Auricularia auricula* and its physicochemical properties. *Food Chem*, 196:486-492. https://doi.org/10.1016/j.foodchem.2015.09.069

Suwannarach N, Kumla J, Watanabe B, et al., 2019. Characterization of melanin and optimal conditions for pigment production by an endophytic fungus, *Spissiomyces endophytica* SDBR-CMU319. *PLoS ONE*, 14(9):e0222187. https://doi.org/10.1371/journal.pone.0222187

Tadokoro T, Kobayashi N, Zmudzka BZ, et al., 2003. UV-induced DNA damage and melanin content in human skin differing in racial/ethnic origin. *FASEB J*, 17(9): 1177-1179. https://doi.org/10.1096/fj.02-0865fje

Tu YG, Sun YZ, Tian YG, et al., 2009. Physicochemical characterisation and antioxidant activity of melanin from the muscles of Taihe Black-bone silky fowl (*Gallus gallus*

*domesticus Brisson*). *Food Chem*, 114(4):1345-1350. https://doi.org/10.1016/j.foodchem.2008.11.015

Walker CA, Gómez BL, Mora-Montes HM, et al., 2010. Melanin externalization in *Candida albicans* depends on cell wall chitin structures. *Eukaryot Cell*, 9(9):1329-1342. https://doi.org/10.1128/EC.00051-10

Wang Y, Aisen P, Casadevall A, 1995. Cryptococcus neoformans melanin and virulence: mechanism of action. *Infect Immun*, 63(8):3131-3136. https://doi.org/10.1128/iai.63.8.3131-3136.1995

Wheeler MH, Bell AA, 1988. Melanins and their importance in pathogenic fungi. *Curr Top Med Mycol*, 2:338-387. https://doi.org/10.1007/978-1-4612-3730-3_10

Wynns AA, Jensen AB, Eilenberg J, 2013. *Ascosphaera callicarpa*, a new species of bee-loving fungus, with a key to the genus for Europe. *PLoS ONE*, 8(9):e73419. https://doi.org/10.1371/journal.pone.0073419

Xu Y, Guo ZJ, 2008. Study on antioxidant activity of extracts from *Aconitum taipeicum*. *Res Pra Chin Med*, 22(1):38-40 (in Chinese). https://doi.org/10.3969/j.issn.1673-6427.2008.01.014

Ye M, Wang Y, Guo GY, et al., 2012. Physicochemical characteristics and antioxidant activity of arginine-modified melanin from *Lachnum* YM-346. *Food Chem*, 135(4):2490-2497. https://doi.org/10.1016/j.foodchem.2012.06.120

Ye M, Guo GY, Lu Y, et al., 2014. Purification, structure and anti-radiation activity of melanin from *Lachnum* YM404. *Int J Biol Macromol*, 63:170-176. https://doi.org/10.1016/j.ijbiomac.2013.10.046

Zaragoza O, Chrisman CJ, Castelli MV, et al., 2008. Capsule enlargement in *Cryptococcus neoformans* confers resistance to oxidative stress suggesting a mechanism for intracellular survival. *Cell Microbiol*, 10(10):2043-2057. https://doi.org/10.1111/j.1462-5822.2008.01186.x

**Supplementary information**

Figs. S1–S8